Supporting Information

Oxidase-like nanozyme-mediated altering the aspect ratio of gold nanorods for breaking through H_2O_2-supported multicolor colorimetric assay: application in the detection of acetylcholinesterase activity and its inhibitors

Ruijie Fu,[†] Jing Zhou,[†] Yiwen Wang,[†] Yanlin Liu,[†] Haoran Liu,[†] Qin Yang,[†] Qiyang Zhao,[†] Bining Jiao, [†] and Yue He *[†]*

[†]Laboratory of Quality & Safety Risk Assessment for Citrus Products (Chongqing), Ministry of Agriculture, Citrus Research Institute, Southwest University, Chongqing, 400712, P.R. China; National Citrus Engineering Research Center, Chongqing, 400712, P.R. China.

* To whom correspondence should be addressed. Dr. Yue He, E-mail: yuehe@cric.cn, Tel: 86-23-68349603, Fax: 86-23-68349046

This file contains:

1. Supporting instruments, reagents and methods

2. Supporting discussions

3. Supporting figures 1-12 with legends

4. Supporting table S1

1. Supporting instruments, reagents and methods

1.1 Instruments. The measurement of the UV-vis absorption spectrum was performed on Varian Cary 50 UV-vis spectrophotometer (Palo Alto, American). The morphology of the synthesized AuNRs was analyzed utilizing a JEM-1200EX transmission electron microscope (TEM, JEOL, Japan). The thickness of the MnO_2 nanosheets was measured by using a dimension icon atomic force microscopy (AFM, Bruker, Germany). The elemental composition and chemical valence of the MnO_2 nanosheets and Mn^{2+} was characterized by utilizing a Thermo Scientific Escalab 250Xi spectrometer (Thermo Scientific, USA). Thermo Scientific CL31R Multispeed centrifuge (Thermo Scientific, USA), Tonson tech Ultrasonic crusher (Shenzhen, China) and Hirayama HVE-50 autoclave (Hirayama, Japan) were used throughout the experiments. The high-resolution X-ray photoelectron spectroscopy analysis of the Mn 2p regions was conducted by using Avantage and all data were evaluated using the Origin 8.0 software.

1.2 Reagents. Acetylcholinesterase (AChE), acetylthiocholine (ATCh), tetramethylammoniam hydroxide (TMA·OH), manganese chloride tetrahydrate ($MnCl_2·4H_2O$), chloroauric acid ($HAuCl_4·4H_2O$), hexadecyl trimethyl ammonium bromide (CTAB), silver nitrate ($AgNO_3$), and ascorbic acid (AA) were all obtained from Sigma-aldrich (Shanghai, China). Sodium borohydride ($NaBH_4$) was obtained from Adamas (Shanghai, China). Lysozyme (Lyz), bovine serum albumin (BSA), hemoglobin (HGB), human serum albumin (HSA), and acid phosphatase (ACP) were all obtained from Solarbio (Beijing, China). 3,3',5,5'-Tetramethylbenzidine (TMB) was obtained from Shanghai Sangon Biotechnology (Shanghai, China). Silver nitrate ($AgNO_3$) was obtained from Acros Organics (Morris Plains, NJ). Acetic acid (HAc) was obtained Chuandong Chemical (Chongqing, China). Anhydrous sodium acetate (NaAc) was purchased from Chengdu Kelon Reagent Chemical Factory (Chengdu, China). Hydrogen peroxide (H_2O_2, 30 wt%) was purchased from Sinopharm Chemical Reagent Co., Ltd (Shanghai, China). The ultra-water uesed in experiments was obtained from a Milli-Q purified system (18.2 MΩ, Millipore, Germany). All chemicals and reagents were used in analytical grade. Buffers put to use in this work are presented as follows:

Tris-HCl buffer (20 mM, pH 6.5); NaAC-HAC buffer (200 mM, pH 4.5).

1.3 Synthesis of the MnO_2 nanosheets. MnO_2 nanosheets were prepared as follows: Tetramethyl ammonium hydroxide (0.6 mol L^{-1}, 18.0 mL), hydrogen peroxide (3 wt%, 2 mL) was prepared in a 100 mL round-bottomed flask. Then, $MnCl_2 \cdot 4H_2O$ (0.3 M, 10 mL) was mixed into the above solution within a period of 15 s. The solution immediately turns dark brown in the mixing process. The resulting dark brown solution was stirred vigorously for 12 hours in the open air at room temperature. Subsequently, the bulk MnO_2 was centrifuged once (10 000 rpm, 10 min), followed by washing with a mixture solution containing ultrapure water and methanol three times. Afterwards, the precipitate was dried in an vacuum freeze drier at a temperature of -20 ℃ for 24 h. The preparation of the MnO_2 nanosheets was accomplished by exfoliating bulk MnO_2 by means of ultrasonication. In general, an ultrasonic cell crusher was put to use for the purpose of degrading 10 mL of 1 mg mL^{-1} MnO_2 suspension last 2 h. Eventually, the supernatant was stored at 4 ℃ following the removal of the unexfoliated MnO_2 through centrifugation at 500 rpm last 5 min.

1.4 Preparation of gold nanorods (AuNRs). AuNRs were prepared by the seed-mediated way. In short, the seed solution was prepared by reduction of $HAuCl_4$ (0.50 mM, 5 mL) with freshly prepared, ice-cold $NaBH_4$ solution (0.01 M, 600 μL) in aqueous CTAB solution (0.20 M, 5 mL). The color of the seed solution changed from yellow to brownish yellow. The vigorous stirring was ceased after 2 min and above solution was aged at 30 ℃ for 2.5 h. For growth solution, the $HAuCl_4$ (1.00 mM, 5 mL) was added to CTAB solution (0.20 M, 5 mL), and then $AgNO_3$ (4.00 mM, 0.25 mL) was injected into the above mixture. After stirring slowly, AA (0.0788 M, 70 μL) was added, and the solution was vigorously stirred for 30 s until it changed from brownish yellow to colorless. Finally, seed solution (12 μL) was quickly injected into the above solution. The resultant mixture was left undisurbed at 30 ℃ for 12 h for AuNRs growth. The prepared AuNRs was concentrated to obtain AuNRs precipitate by centrifuging at 10000 rpm for 15 min. The precipitates stored in room temperature for next use.

2. Supporting discussions

Characterization of the MnO_2 nanosheets. The ultrathin MnO_2 nanosheets were systematically characterized by TEM, AFM, X-ray photoelectron spectroscopy (XPS) and UV-vis spectroscopy. As shown in Figure S4, the as-prepared MnO_2 nanosheets showed a representative two-dimensional sheet-like morphology with a lateral size of several hundreds of nanometers. This result set forth the fact that MnO_2 nanosheets have large surface areas, which are equipped to provide more active sites for the catalytic reaction of TMB. In the AFM images the MnO_2 showed the uniform thickness of 1.0 nm (Figure S5). Meanwhile, the obtained MnO_2 nanosheets solution was brown with a characteristic absorption peak at 360 nm (Figure S6), which is consistent with the d-d transition of Mn^{4+} ions. Figure S7 displays the full scan XPS spectrum of MnO_2 nanosheets. The typical binding energy peaks of MnO_2 nanosheets that correspond to Mn 2p, O 1s, N 1s and C 1s were evidently observed at 642.3, 525.5, 402.6 and 286.3 eV, correspondingly (Figure S7A). The high resolution XPS spectrum of the Mn 2p regions exhibited two peaks centered at 642.3 eV and 654.0 eV, belonging to Mn2p3/2 and Mn2p1/2, respectively (Figure S7B). All the above results demonstrated that the ultrathin MnO_2 nanosheets were successfully prepared.

3. Supporting figures 1–12 with legends

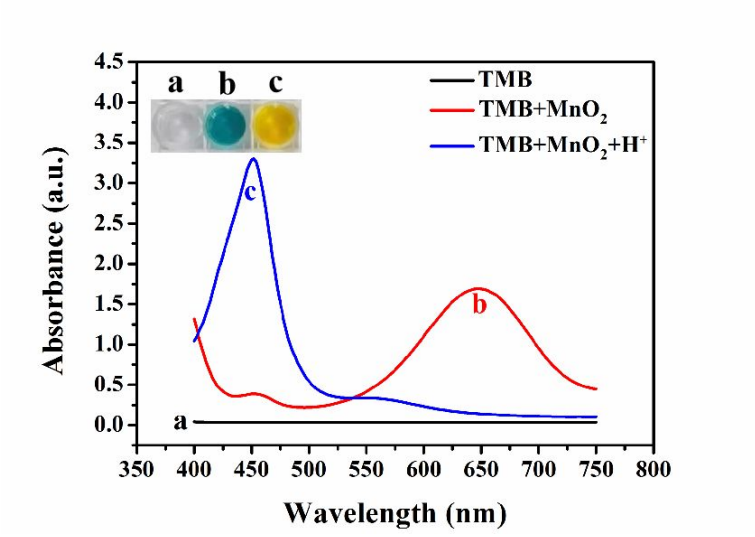

Figure S1. UV−vis absorption spectra of (a) TMB (b) MnO_2 + TMB (c) MnO_2 + TMB + H^+ (inset: the corresponding photographs).

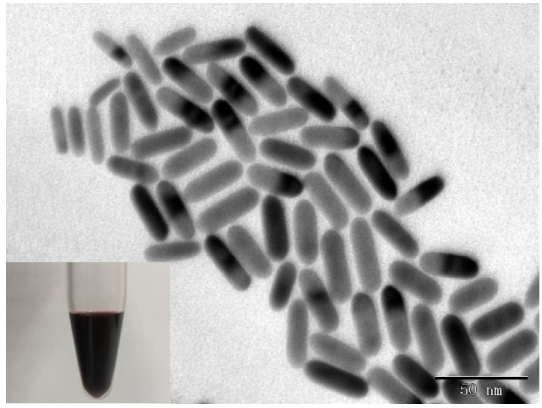

Figure S2. TEM image of AuNRs (inset: the corresponding photographs).

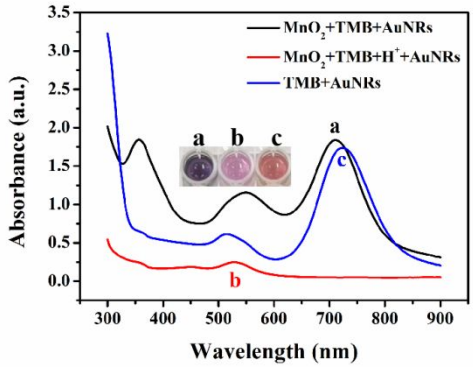

Figure S3. UV−vis absorption spectra of (a) MnO_2 + TMB +AuNRs (b) MnO_2 + TMB + H^+ + AuNRs and (c) TMB + AuNRs (inset: the corresponding photographs).

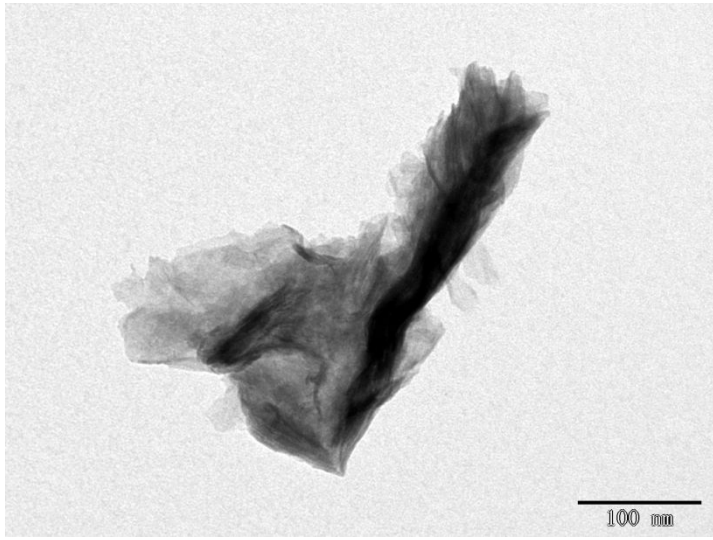

Figure S4. TEM image of MnO_2 nanosheets.

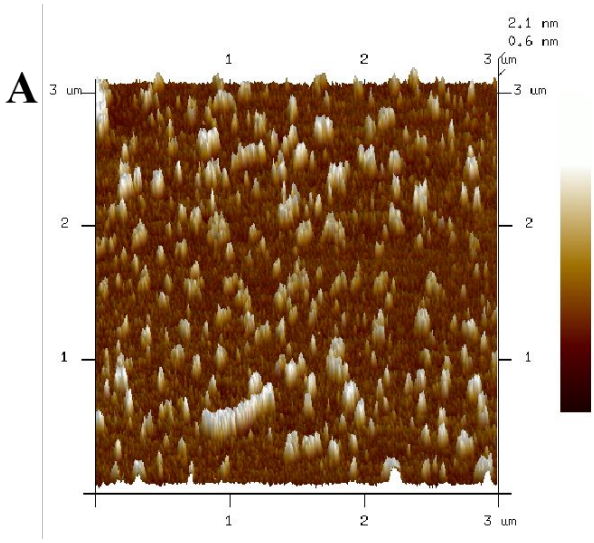

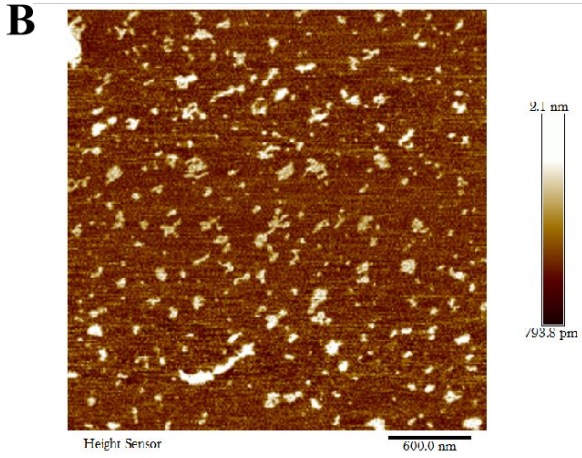

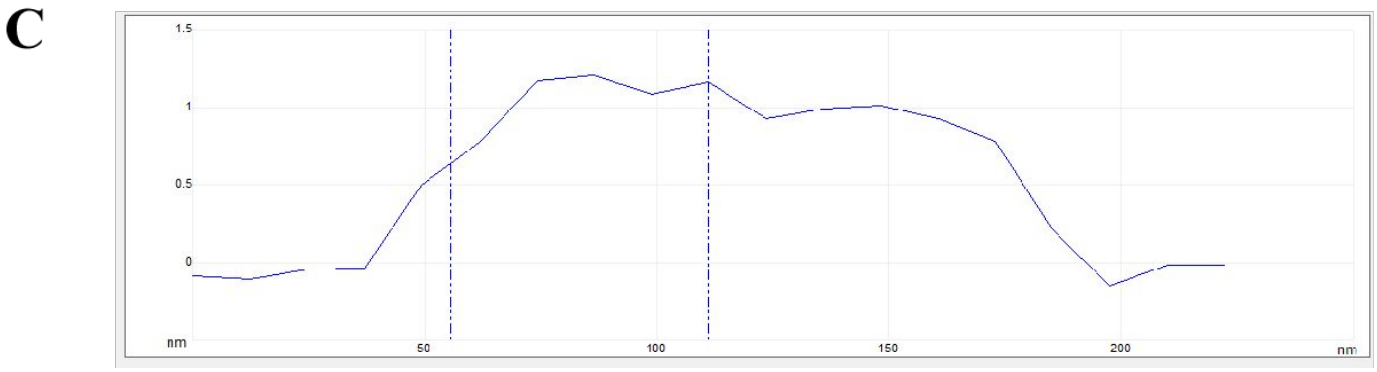

Figure S5. (A) 3D- AFM image of the MnO_2 nanosheets, (B) AFM image of the MnO_2 nanosheets, and (C) Height profile along a white line overlaid on the AFM image.

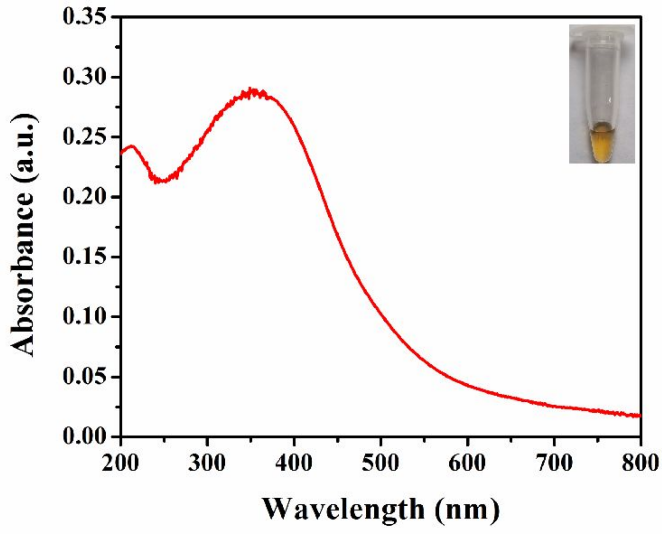

Figure S6. UV−vis absorption spectra of MnO_2 nanosheets (inset: the corresponding photographs).

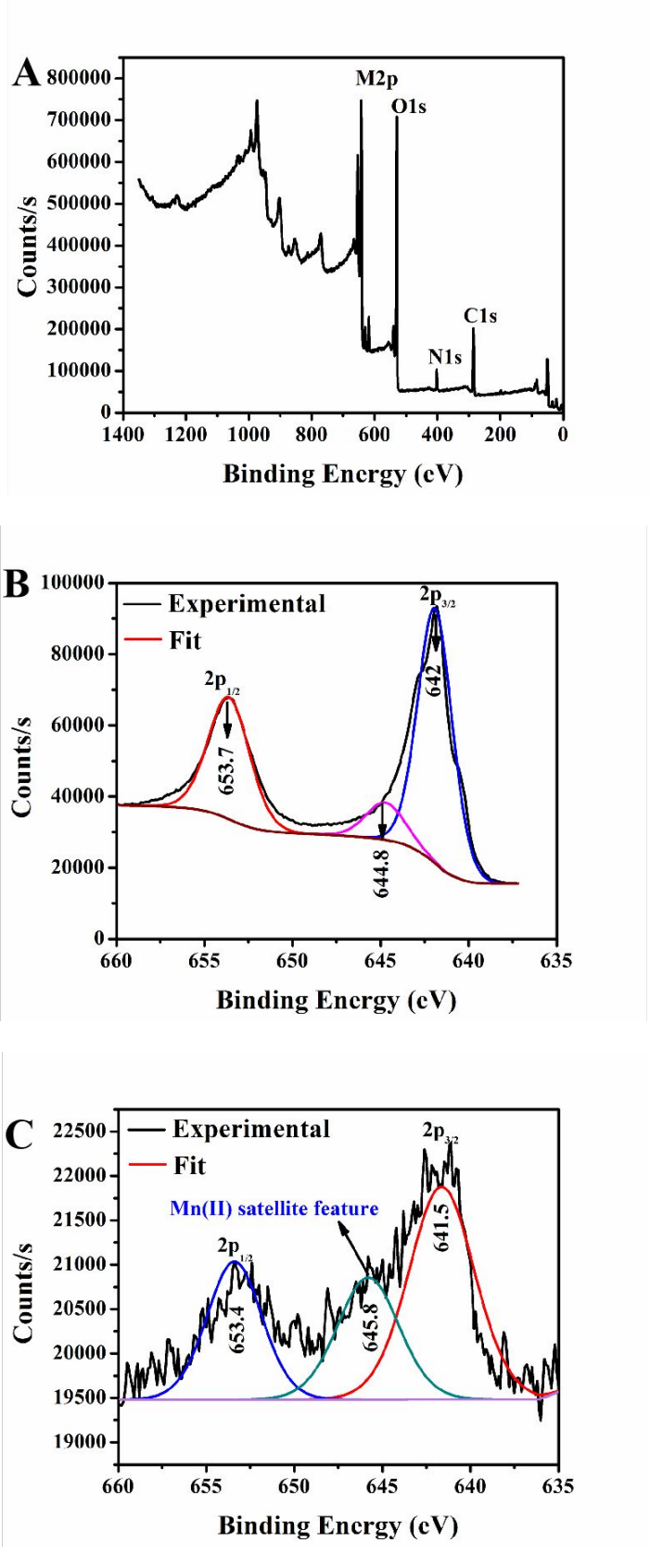

Figure S7. XPS spectra of MnO_2 nanosheets. (A) Wide scan and (B) Mn 2p spectra. (C) Mn 2p spectra of MnO_2 nanosheets + (AChE +ATCh).

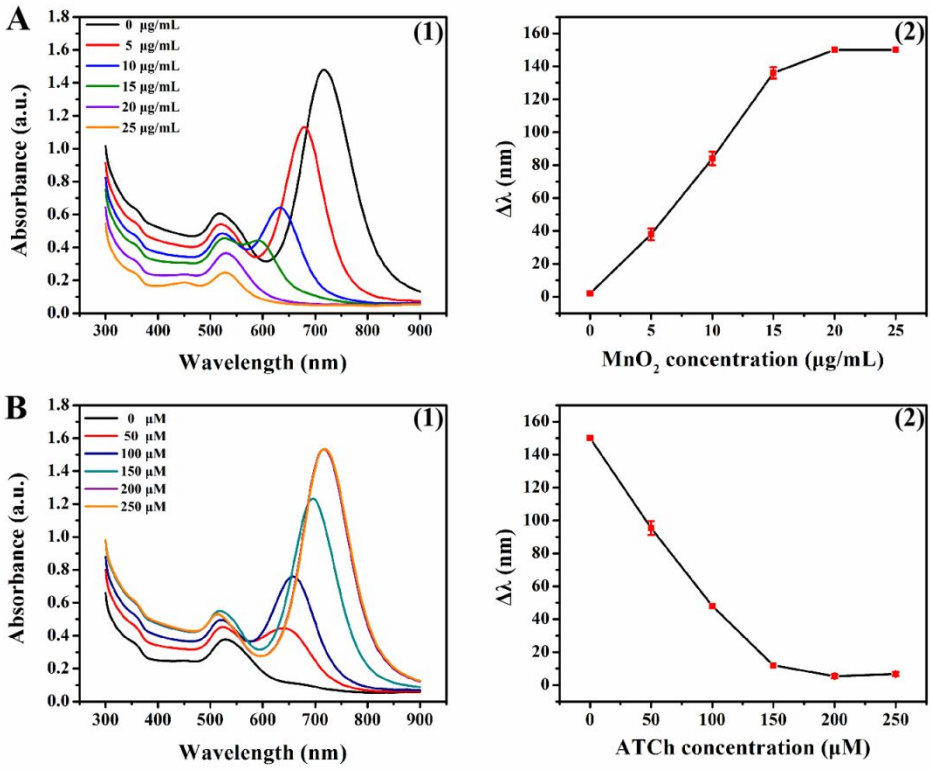

Figure S8. Effect of different reaction conditions on Δλ. (A) MnO_2 concentrations, (B) ATCh concentrations. Error bars represent the standard error derived from three repeated measurements (n=3).

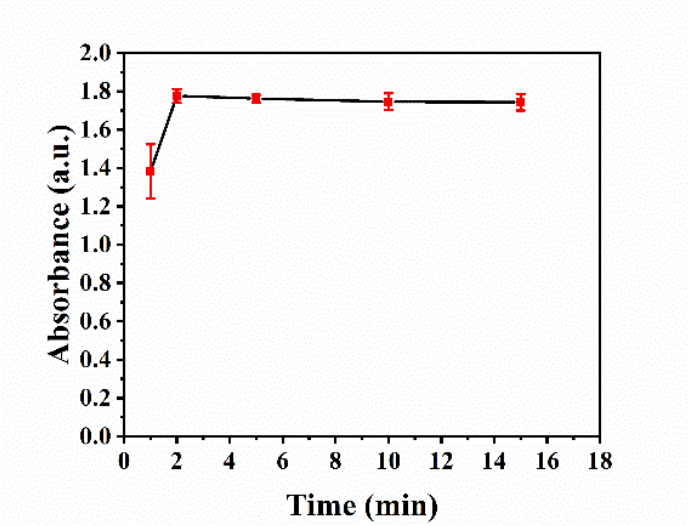

Figure S9. The absorbance responses of MnO_2-TMB system under different incubation time. Error bars represent the standard error derived from three repeated measurements (n=3).

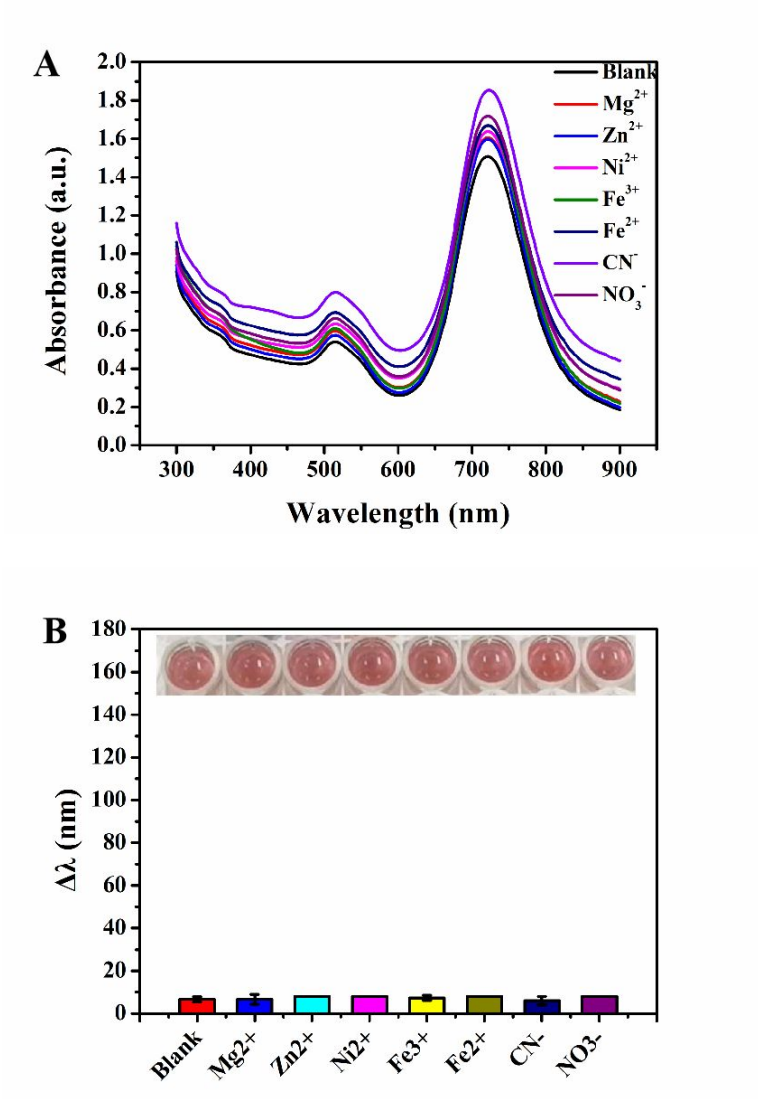

Figure S10. (A) UV−vis absorption spectra and (B) Longitudinal LSPR peak shift of AuNRs responding to different ions (60 nM for Mg^{2+}, Zn^{2+}, Ni^{2+}, Fe^{3+}, Fe^{2+}, CN^-, and NO_3^-). Inset: the corresponding color of the colorimetric platform after adding different ions. Error bars represent the standard error derived from three repeated measurements (n=3).

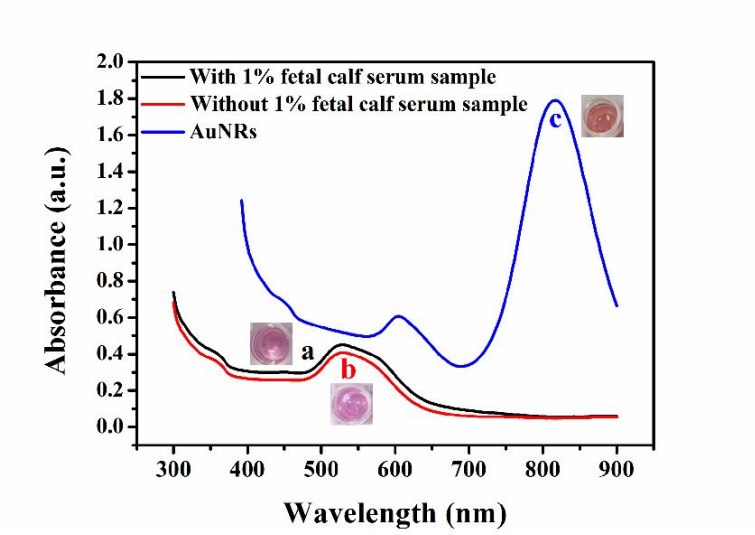

Figure S11. UV−vis absorption spectra of AuNRs under different conditions. (a) MnO_2 nanosheets-mediated etching of AuNRs in the presence of 1% fetal calf serum sample. (b) MnO_2 nanosheets-mediated etching of AuNRs in the absence of 1% fetal calf serum sample. (c) AuNRs. The inset pictures show the colors of the corresponding solutions.

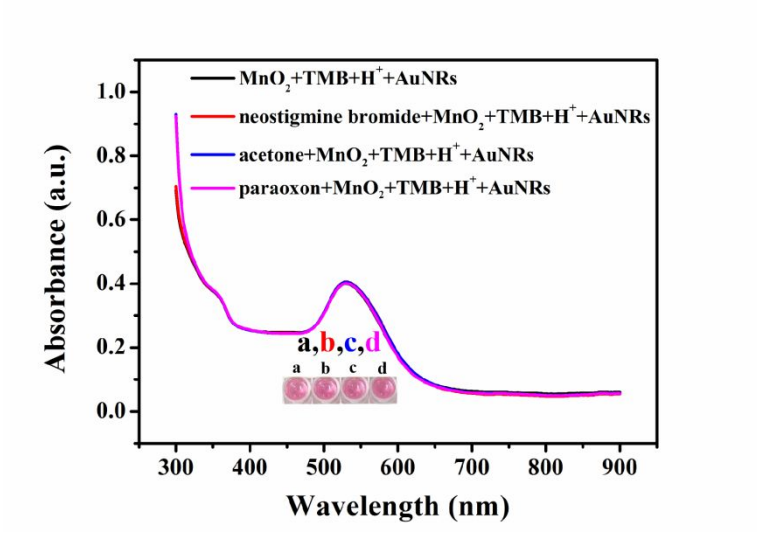

Figure S12. The influence of neostigmine bromide and paraoxon on MnO_2+TMB system. UV−vis absorption spectra of (a) MnO_2 + TMB + H^+ + AuNRs (b) neostigmine bromide + MnO_2 + TMB + H^+ + AuNRs (c) acetone + MnO_2 + TMB + H^+ + AuNRs (d) paraoxon + MnO_2 + TMB + H^+ + AuNRs (inset: the corresponding photographs).

4. Supporting table S1

Table S1. Comparison of the proposed platform with other platform for AChE detection.

Nanomaterials	Linear range (mU/mL)	LOD (mU/mL)	Color changes	Refs.
Cobalt oxyhydroxide nanoflakes	0.05–20	0.033	Single color	1
MnO_2 nanosheets	0.1–15	0.035	Single color	2
Prussian blue nanocubes	0.1–5.0	0.04	Single color	3
Polyacrylic acid-coated cerium oxide nanoparticles	0–50	0.263	Single color	4
γ -MnOOH nanowires	0.01–1.25	0.007	Single color	5
Fe_3O_4 magnetic nanoparticle	–	–	Single color	6
MnO_2 nanosheets	25–500	0.18	Multicolor	This work

Reference

1. Jin, R.; Xing, Z. H.; Kong, D. S.; Yan, X.; Liu, F. M.; Gao, Y.; Sun, P.; Liang, X. S.; Lu, G. Y. Sensitive colorimetric sensor for point-of-care detection of acetylcholinesterase using cobalt oxyhydroxide nanoflakes. *J. Mater. Chem. B* **2019**, *7*, 1230-1237.

2. Yan, X.; Song, Y.; Wu, X. L.; Zhu, C. Z.; Su, X. G.; Du, D.; Lin, Y. H. Oxidase-mimicking activity of ultrathin MnO_2 nanosheets in colorimetric assay of acetylcholinesterase activity. *Nanoscale* **2017,** *9* (6), 2317-2323.

3. Ni, P. J.; Sun, Y. J.; Dai, H. C.; Lu, W. D.; Jiang, S.; Wang, Y. L.; Li, Z.; Li, Z., Prussian blue nanocubes peroxidase mimetic-based colorimetric assay for screening acetylcholinesterase activity and its inhibitor. *Sensor Actuat. B-Chem.* **2017**, *240*, 1314-1320.

4. Zhang, S. X.; Xue, S. F.; Deng, J. J.; Zhang, M.; Shi,G. Y.; Zhou, T. S. Polyacrylic acid-coated cerium oxide nanoparticles: An oxidase mimic applied for colorimetric assay to organophosphorus pesticides. *Biosens. Bioelectron.* **2016**, *85*, 457-463.

5. Huang, L. J.; Sun, D. W.; Pu, H. B.; Wei, Q. Y.; Luo, L. P.; Wang, J. L. A colorimetric paper sensor based on the domino reaction of acetylcholinesterase and degradable γ-MnOOH nanozyme for sensitive detection of organophosphorus pesticides. *Sensor Actuat. B-Chem.* **2019**, *290*, 573-580.

6. Liang, M. M.; Pan, Y.; Jiang, H.; Wang, F.; Yang, D. L.; Lu, D.; Feng, J.; Zhao, J. J.; Yang, L.; Yan, X. Y. Fe_3O_4 Magnetic Nanoparticle Peroxidase Mimetic-Based Colorimetric Assay for the Rapid Detection of Organophosphorus Pesticide and Nerve Agent. *Anal. Chem.* **2012**, *85*, 308-312.